The Role of Intraalveolar Fibrosis in the Process of Pulmonary Structural Remodeling in Patients With Diffuse Alveolar Damage

YUH FUKUDA, MD, PhD, MASAMICHI ISHIZAKI, PhD, YUKINARI MASUDA, BS, GO KIMURA, MD, OICHI KAWANAMI, MD, PhD, and YOZO MASUGI, MD, PhD

From the Department of Pathology, Nippon Medical School, Tokyo, Japan

For a study of the processes and mechanisms of pulmonary structural remodeling in fibrotic lungs and metaplastic squamous epithelial cells in fibrotic alveoli, immunohistochemical, ultrastructural, and light-microscopic morphometric observations were made of the lungs in acute and proliferative stages of diffuse alveolar damage (n = 40) obtained from biopsies and autopsies. Morphometry showed that intraalveolar fibrosis developed in the early proliferative stage and was more prominent than interstitial fibrosis. In the early proliferative stage, activated myofibroblasts migrated into intraalveolar spaces through gaps in the epithelial basement membrane. They then attached to the luminal side of epithelial basement membrane and produced intraalveolar fibrosis and coalescence of alveolar walls. This intraalveolar fibrosis was the essential factor in the remodeled lungs. Albumin, fibrinogen, immunoglobulins, and surfactant apoprotein were present throughout the hyaline membrane. Fibronectin was not found in hyaline membrane of the lesions in early acute stage but was demonstrated in later stages in outer layers of hyaline membranes and in the areas of intraalveolar fibrosis. Fibronectin may be responsible for the migration and proliferation of myofibroblasts in intraalveolar spaces. Metaplastic single-layered and stratified squamous epithelial cells were keratin-positive and surfactant apoprotein-negative. These metaplastic epithelial cells were frequently found in the alveoli with minimal Type II epithelial cell proliferation and in the grossly scarred alveoli. (Am J Pathol 1987, 126:171-182)

A MORPHOLOGIC characteristic of fibrotic lung disorders is the remodeled pulmonary structure with deposits of fibrous tissue in the lung. The remodeled fibrotic alveolar walls are frequently lined by increased numbers of Type II alveolar epithelial cells and cuboidal and squamous metaplastic cells.[1-3] There are two types of changes in fibrotic lung disorders: interstitial and intraalveolar fibrosis.[2,4,5] In experimental paraquat-treated lungs[6] intraalveolar fibrosis is more important than interstitial fibrosis in the remodeling of the pulmonary structure, because intraalveolar fibrosis results in obliteration of alveoli, coalescence of alveolar walls, and loss of functional alveolar-capillary units. On the other hand, it is not easy to study the early and intermediary processes of pulmonary structural remodeling in patients with fibrotic lung disorders, because of the inability to perform serial lung biopsies in a single patient and the difficulties in obtaining samples of the early stages of lung fibrosis.

Diffuse alveolar damage (DAD) is the usual underlying abnormality in patients with the adult respiratory distress syndrome (ARDS), and it is known that a fibrotic change occurs in the early stages of the disease.[7] To examine the importance of intraalveolar fibrosis in the process of pulmonary structural remodeling in human fibrotic lungs and to analyze the mechanisms in the formation of intraalveolar fibrosis and metaplastic epithelium in alveoli, we studied lung specimens obtained from autopsies and biopsies of acute and proliferative stages of clinically diagnosed

Accepted for publication August 27, 1986.

Address reprint requests to Dr. Yuh Fukuda, Department of Pathology, Nippon Medical School, 1-1-5 Sendagi, Bun-kyo-ku, Tokyo 113, Japan.

ARDS by electron microscopy, immunohistochemistry, and light-microscopic morphometry.

Materials and Methods

Lung tissues from 3 biopsies and 37 autopsies of cases of DAD with clinical diagnosis of ARDS and 3 control cases were investigated. The lung tissues were obtained from patients who had a history of severe dyspnea of from 1 to 40 days. All patients were treated by artificial ventilator and a high concentration of oxygen. The underlying diseases of ARDS were massive hemorrhages (4 cases), burn (7 cases), rupture of the alimentary tract (3 cases), pancreatic necrosis (2 cases), liver disease (2 cases), chronic renal failure (2 cases), cerebral apoplexy (2 cases), emphysema (1 case), paraquat toxicity (1 case), formaldehyde toxicity (1 case), and malignant tumor (14 cases). In 7 cases sepsis had occurred during the clinical course. Seven patients with malignant tumor had foci of bacterial infection. Eight patients with malignant tumor were treated with antineoplastic drugs. All biopsy specimens were obtained at the time of the operation for pneumothorax caused by the artificial ventilator. Control lung tissues were obtained from normal areas of lungs surgically removed for cancer.

Histologic Evaluation

The lungs of autopsy cases were fixed by immersion, via the airways, with 15% formalin solution. The lungs of biopsy cases were fixed immediately by perfusion, with 15% formalin solution. Selected blocks of tissues were embedded in paraffin. Histologic sections of paraffin-embedded tissues were stained with hematoxylin and eosin (H&E), Masson trichrome, elastica van Gieson (EVG), elastica Masson trichrome, and periodic acid–methenamine silver (PAM).

Immunofluorescence Methods for Detection of IgG, IgM, IgA, Albumin, and C3

Unfixed tissue blocks of 15 cases of DAD and 3 control cases were frozen in dry ice–acetone and were stored at −70 C. Frozen sections were cut at a thickness of 4 μ and air-dried. These sections were then incubated for 30 minutes at room temperature with normal goat serum at a dilution of 1:20 in phosphate-buffered saline (PBS). The sections were washed with PBS and incubated for 30 minutes at room temperature with an appropriate dilution of the following: rabbit anti-human IgG, IgM, IgA, or C3 antibodies (Cappel Laboratories). After washing three times with PBS, the sections were incubated for 30 minutes at room temperature with fluorescein isothiocyanate-labeled goat anti-rabbit IgG (Cappel Laboratories) at 1:20 dilution, washed three times with PBS, coverslipped in buffered glycerol, and observed under a fluorescence microscope.

Immunoperoxidase Methods for Detection of Fibronectin, Fibrinogen, Keratin, and Pulmonary Surfactant Apoprotein

Paraffin-embedded tissue sections were cut at a thickness of 3 μ and mounted on precleaned glass slides without adhesives. Deparaffinized, rehydrated tissue sections were washed three times with PBS and treated with 0.3% hydrogen peroxide in methanol for 30 minutes for elimination of endogenous peroxidase activity. After three washes with PBS, the tissue sections were treated with 0.1% protease, Type VII (Sigma Chemical Co.) in 0.1 M phosphate buffer, for 10 minutes for unmasking the antigenic sites. Then the sections were washed three times with PBS and incubated for 30 minutes at room temperature with normal swine or goat serum at a dilution of 1:20 in PBS for blocking nonspecific antibody reactions. For the detection of fibronectin, this step was omitted because the fibronectin in normal serum might cause false-positive reactions.[8] The sections were then incubated for 30 minutes at room temperature either with rabbit anti-human fibronectin antibody (DAKO, Denmark) at a dilution of 1:400, rabbit anti-human fibrinogen antibody (DAKO, Denmark) at a dilution of 1:40, or rabbit anti-human epidermal keratin antibody (DAKO, Denmark) at a dilution of 1:160 or mouse monoclonal antibody against human pulmonary surfactant apoprotein (PE 10) (provided by Drs. Kuroki and Akino) at a dilution of 1:500.

The specificity of antifibronectin antibody was confirmed by immunoelectrophoresis, in which antifibronectin antibody formed a single precipitation band with both plasma and purified fibronectin from plasma obtained from a gelatin–Sepharose 4B column.[9] No band was formed with plasma components from which fibronectin had been removed. The specificity of the antibody PE 10 was confirmed by Western blotting.[10]

After washing three times with PBS for 15 minutes, the tissue sections were incubated for 30 minutes at room temperature with peroxidase-labeled swine anti-rabbit IgG antibody (DAKO, Denmark) at a dilution of 1:60 or peroxidase-labeled goat anti-mouse IgG antibody (Fab) (Medical Biological Laboratory, Japan) at a dilution of 1:45 and washed three times with PBS for 15 minutes. The sections were then reacted with a solution of 3,3′-diaminobenzidine

(DAB) and hydrogen peroxide for 2–7 minutes,[11] washed with water, counterstained with Mayer's hematoxylin, dehydrated, and mounted.

Transmission Electron Microscopic Study

For the transmission electron microscopic study, tissues fixed by perfusion with formaldehyde were cut into 1-mm cubes, washed in several changes of 0.1 M phosphate buffer, pH 7.2, and fixed with 2% glutaraldehyde in 0.1 M phosphate buffer. Tissue blocks from biopsy cases and some autopsy cases were fixed immediately after removal with 2% glutaraldehyde solution. Tissue blocks were washed with several changes of phosphate buffer and postfixed with 1% OsO_4 in phosphate buffer, dehydrated, and embedded in Epon 812. For direct correlation, semithin sections were cut and stained with alkaline toluidine blue and observed with a light microsope. Ultrathin sections were stained either with uranyl acetate and lead citrate or, for evaluation of elastic fibers, with tannic acid[12] and examined with a Hitachi H800 electron microscope.

Light-Microscopic Morphometric Study

For light-microscopic morphometry, 2 control cases and 15 DAD cases were used to clarify each of the tissue areas of interstitium of alveolar walls and intraalveolar fibrosis. Ten random areas of alveoli of PAM-stained slides of each case were studied at a magnification of ×50, by a Carl Zeiss Micro-video MAT II computerized image analyzer (West Germany). The interstitial areas of alveolar walls and the areas of intraalveolar fibrosis were measured and recorded as a percentage of the total area. The vascular lumens were not measured. The intraalveolar fibrosis interstitium area ratio of each case was calculated.

Although the PAM stain is useful in detecting the epithelial basement membrane and helps in defining the border of the original intraalveolar spaces and alveolar walls,[13] in the cases of the remodeled stage, it is difficult to distinguish intraalveolar fibrosis from interstitial fibrosis; therefore, the total tissue areas including interstitium and intraalveolar fibrosis were measured. The areas of hyaline membrane were not measured in this study.

Results

By light-microscopic study, the lesions were divided into three stages: acute (14 cases), early proliferative (22 cases), and remodeled (4 cases). The detailed findings of lungs in control cases and each stage of the lesions were as follows.

Control Cases

Light-microscopic study of lungs in control cases showed thin alveolar walls and a few intraalveolar macrophages. Immunohistochemical studies showed fibronectin mainly in the basal layer of endothelial cells of alveolar walls and bronchi. Fibrinogen, IgG, IgM, IgA, and albumin were observed only in the intravascular plasma. C3 was not detected. Keratin was found in the basal cells of bronchi, bronchial glands, and mesothelial cells. Alveolar epithelial cells were negative for keratin. Pulmonary surfactant apoprotein was found in the cytoplasm of Type II alveolar epithelial cells and the cuboidal cells, which were located between the ciliated cells at the peripheral portions of bronchioles. Transmission electron-microscopic study showed a normal arrangement of alveolar and bronchial epithelial cells, vessels, and interstitial connective tissue components.

Acute Stage

Light-microscopic study of the acute stage showed alveolar edema and hyaline membrane formation. Hyaline membranes were formed mainly in alveolar ducts but in some cases were found diffusely on alveolar walls. The results of the immunohistochemical study of hyaline membrane in this and following stages are summarized in Table 1. IgG (Figure 1) and fibrinogen (Figure 2) were strongly and diffusely positive in hyaline membrane. IgA, IgM, and albumin were only weakly positive in the hyaline membrane. C3 was negative or trace-positive in hyaline membrane. Pulmonary surfactant apoprotein was detected in Type II alveolar epithelial cells and some areas of hyaline membranes (Figure 3). Fibronectin was detected mainly on the surfaces of hyaline membrane and on some alveolar surfaces in addition to the basal layer of endothelial cells (Figure 4), although it was not detected in early lesions of this stage. Keratin was found in basal cells of the bronchial epithelia, bron-

Table 1 — Immunohistochemical Findings of Hyaline Membranes in Each Stage of DAD

	Acute stage		Early proliferative stage	Remodeled stage
	Early	Late		
Albumin	+	+	+	+
IgG	+	+	+	+
IgM	+	+	+	+
IgA	+	+	+	+
C3	−	−	−	−
Fibronectin	−	+*	+*	+*
Fibrinogen	+	+	+	+
Surfactant	+&−	+&−	+&−	+&−

*Outer layers of hyaline membranes are positive.

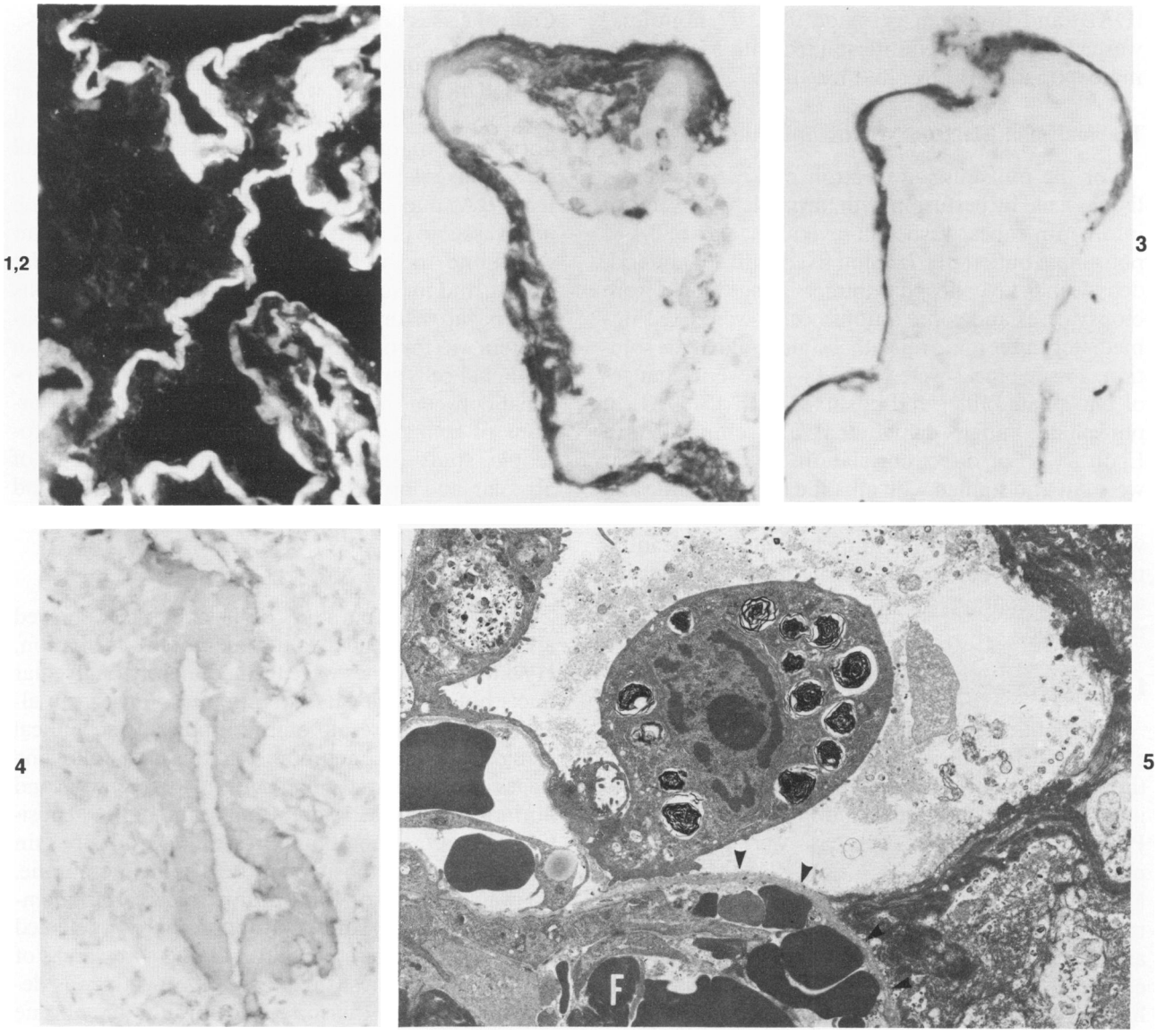

Figure 1—Acute stage. Fluorescence micrograph showing intense IgG staining in hyaline membrane. (Immunofluorescence, ×150) **Figure 2**—Acute stage. Fibrinogen staining is demonstrated in hyaline membrane. (Immunoperoxidase. ×350) **Figure 3**—Acute stage. Surfactant apoprotein staining frequently detected in hyaline membrane, as shown in this figure. (Immunoperoxidase, ×350) **Figure 4**—Acute stage. Fibronectin staining predominantly found on the surfaces of hyaline membrane. (Immunoperoxidase, ×300) **Figure 5**—Acute stage. Epithelial basement membrane partially covered with Type II epithelial cells. The remaining portion of epithelial basement membrane *(arrowheads)* has been denuded and partially covered with hyaline membrane. Alveolar wall shows denuded capillary basement membrane, fibrin thrombus *(F)* in capillary, and extravasation of erythrocytes. (×3700)

chial glands, and mesothelial cells. Some Type II alveolar epithelial cells were weakly positive for keratin.

The electron-microscopic study showed diffuse alveolar epithelial cell damage and a widely denuded epithelial basement membrane of the alveolar walls. Occasionally, activated Type II alveolar epithelial cells were found beneath the hyaline membrane (Figure 5). The hyaline membrane showed fine granular and filamentous structures associated with strands of fibrin and cellular debris. Occasional fibrin thrombi

Figure 6—Early proliferative stage. Many activated interstitial cells in alveolar walls are seen. Hyaline membrane is occasionally found *(arrowheads)*. (H&E, ×300) **Figure 7**—Early proliferative stage. Diffuse intraalveolar fibrosis *(asterisks)* are clearly found in PAM-stained tissue. *Arrowheads* show PAM-positive epithelial basement membranes, which make a borderline between intraalveolar fibrosis and alveolar wall. (PAM, ×150) **Figure 8**—Early proliferative stage. Fibronectin staining predominantly found on the surfaces of hyaline membrane *(asterisks)* and areas of intraalveolar fibrosis. (Immunoperoxidase, ×300) **Figure 9**—Early proliferative stage. Regenerating epithelial cells covering intraalveolar fibrosis *(IF)* show strongly positive staining for keratin. (Immunoperoxidase, ×250) **Figure 10**—Early proliferative stage. Epithelial cells having cytoplasmic hyaline show positive keratin staining in their cytoplasms. (Immunoperoxidase, ×450) **Figure 11**—Early proliferative stage. Epithelial cells having cytoplasmic hyaline *(arrowheads)* show negative surfactant apoprotein stainings. Type II alveolar epithelial cells are heavily positive. (Immunoperoxidase, ×450) **Figure 12**—Early proliferative stage. Epithelial basement membrane is widely denuded *(arrowheads)*, and two activated myofibroblasts are seen in edematous alveolar wall. (×5400)

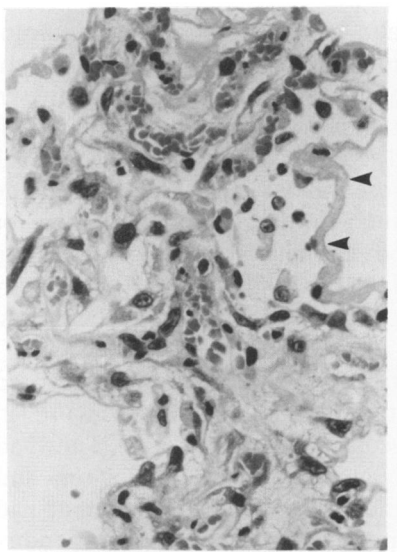

6,7

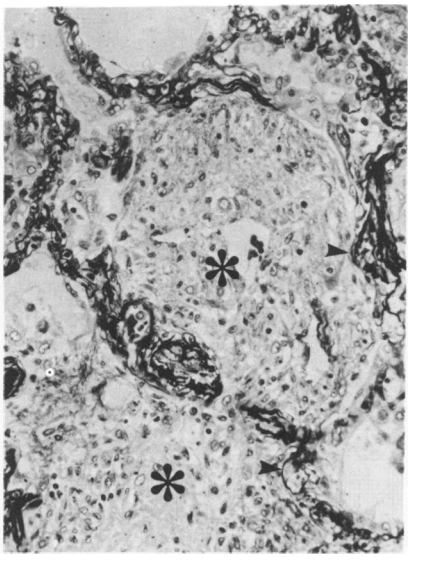

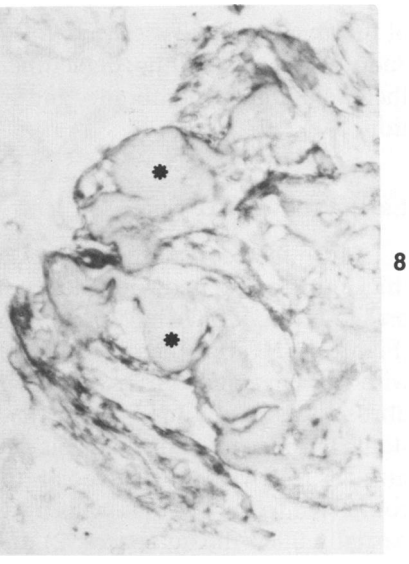

8

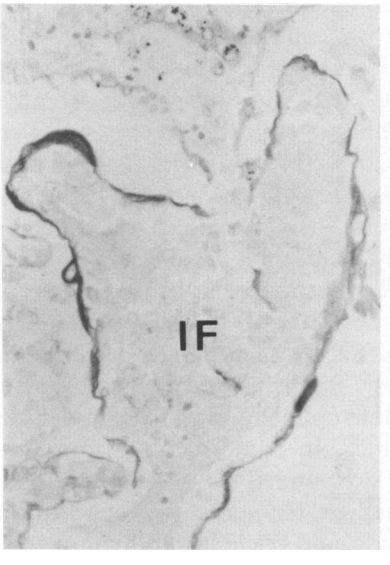

9,10

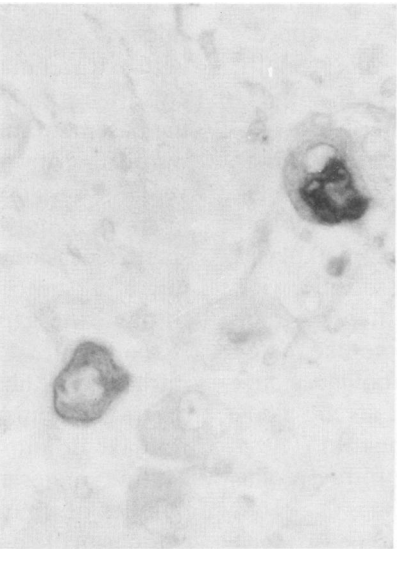

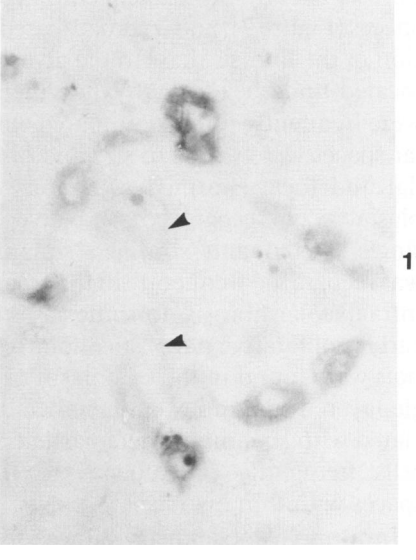

11

12

of the alveolar capillaries were found associated with endothelial cell swelling, detachment from the endothelial basement membrane, and neutrophil infiltration.

Early Proliferative Stage

Light-microscopic study showed alveolar wall thickening associated with edema and interstitial cell proliferation, which have large nuclei and nucleoli (Figure 6). Hyaline membrane formations associated with intraalveolar fibrosis were found. Intraalveolar fibrosis was easily observed in the slides with PAM stain. Three types of intraalveolar fibrosis were recognized as follows: 1) intraalveolar "buds," which were connected to the alveolar walls by a narrow stalk and partially filled the air spaces; 2) diffuse intraalveolar fibrosis, which obstructed completely the alveolar spaces (Figure 7); and 3) broad-based areas of apposition of the fibrosis mass to the alveolar walls, usually located underneath the hyaline membrane (2 and 3 were frequently found, compared with 1). The alveolar spaces were varied in size and obliterated. Cuboidal and focal stratified squamous epithelial metaplasia was recognized on alveolar walls, and single-layered and stratified squamous metaplasia was recognized frequently in the areas associated with intraalveolar fibrosis. In some cases (3 of 22 cases of early proliferative stage), alcoholic hyaline-like materials were found in the cytoplasm of cuboidal or single-layered squamous epithelial cells of alveoli associated with squamous metaplastic epithelium. These cells frequently protruded into the intraalveolar spaces with thin cytoplasm.

Immunohistochemistry showed IgG to be strongly positive in hyaline membrane and IgM, IgA, and albumin to be weakly positive, similar to the situation in the acute stage. Fibrinogen was located in the hyaline membrane and fibrin strands in some intraalveolar spaces and intravascular spaces. Fibronectin was found more predominantly on the outer zones of hyaline membrane, compared with the previous stage and in the areas of intraalveolar fibrosis (Figure 8). Keratin was positive in the single-layered and stratified squamous and cuboidal epithelium of alveoli in addition to basal cells of bronchial epithelium, bronchial glands, and mesothelium. Type II alveolar epithelial cells were increased and weakly positive to anti-keratin antibody. Most of the newly regenerated metaplastic epithelium covering intraalveolar buds were strongly keratin-positive (Figure 9), but pulmonary surfactant apoproteins were negative. Pulmonary surfactant apoprotein was strongly positive in granular materials and hyaline membranes in intraalveolar spaces and associated with Type II alveolar epithelial cells and cuboidal cells. The cells having cytoplasmic hyaline showed a positive reaction for antikeratin antibody in their cytoplasm surrounding the hyaline materials (Figure 10), but pulmonary surfactant apoprotein was always negative in these cells. (Figure 11).

The electron-microscopic study showed activated myofibroblasts in the alveolar interstitium (Figure 12) and some intraalveolar spaces (Figure 13). They had well-developed rough endoplasmic reticulum and large nuclei and nucleoli. Myofibroblasts that had migrated into the intraalveolar spaces had perpendicularly arranged actinlike filaments in their cytoplasmic processes that were aligned in a colinear fashion with extracellular filaments (fibronectin) on the cellular surfaces and attached to the luminal side of epithelial basement membrane or fibrin (Figure 14). There were some newly formed collagen fibrils in intraalveolar spaces associated with myofibroblasts. Elastic fibers were not found in intraalveolar spaces in this stage. Occasionally, some myofibroblasts were seen migrating into the intraalveolar spaces, passing through the gaps of the epithelial basement membrane (Figure 15). The epithelium surrounding the intraalveolar fibrosis frequently showed single-layer or stratified squamous epithelium, which had well-developed desmosomes. In some cases, cytoplasmic hyaline material surrounded with well-developed bundles of intermediate filaments was found in the cytoplasm of cuboidal and single-layer squamous epithelial cells of the alveoli.

Remodeled Stage

Light-microscopic study showed lesions of fibrotic and obliterated alveoli. Alveolar walls showed irregularity in thickness and were covered by single-layer and stratified squamous and cuboidal epithelium, associated with irregular dilatation and narrowing of alveolar spaces. EVG and elastica Masson trichrome stains showed that fibrotic lesions consisted of obliterations of alveoli resulting from intraalveolar fibrosis (Figure 16). Other less fibrotic alveoli, in some cases, showed superimposed newly formed hyaline membranes and the early organization of intraalveolar ex-

Figure 13—Early proliferative stage. Myofibroblast within intraalveolar space attaches to the luminal side of denuded epithelial basement membrane. (×9300) **Figure 14**—High magnification of the area from Figure 13 showing the fine extracellular filaments *(arrowheads)* between the cytoplasmic processes of myofibroblasts and the luminal side of epithelial basement membrane. (×28,000) **Figure 15**—Early proliferative stage. A myofibroblast is passing through the gap *(arrowheads)* of epithelial basement membrane into the intraalveolar space (×9100)

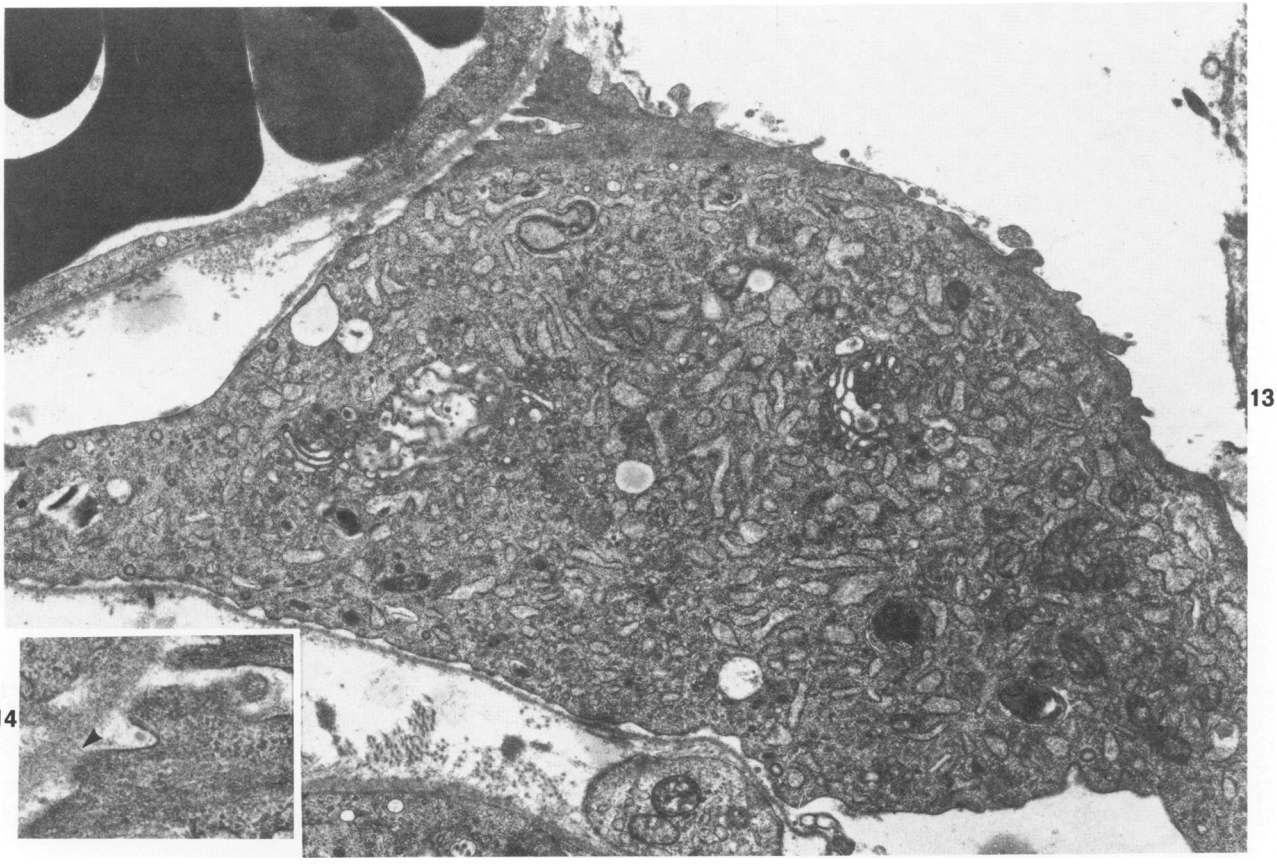

13

14

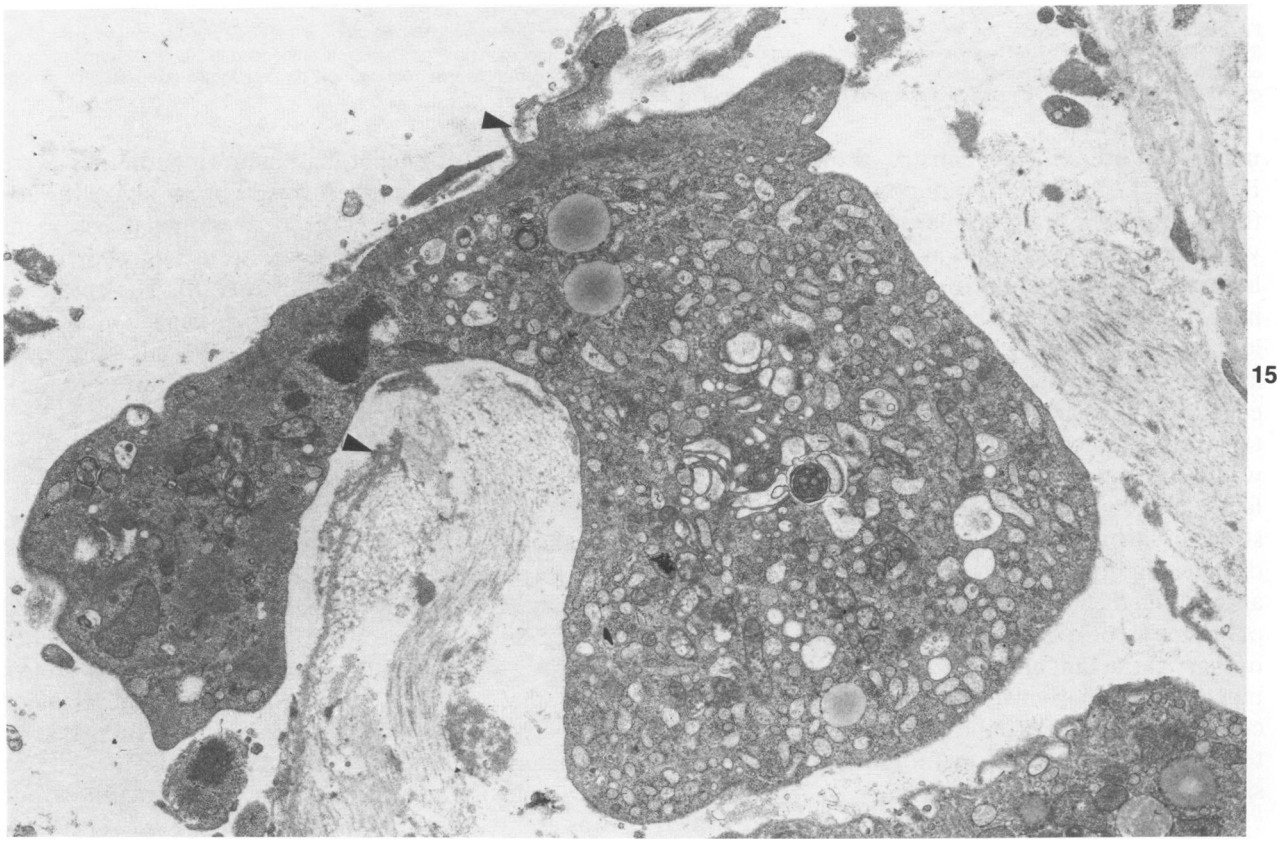

15

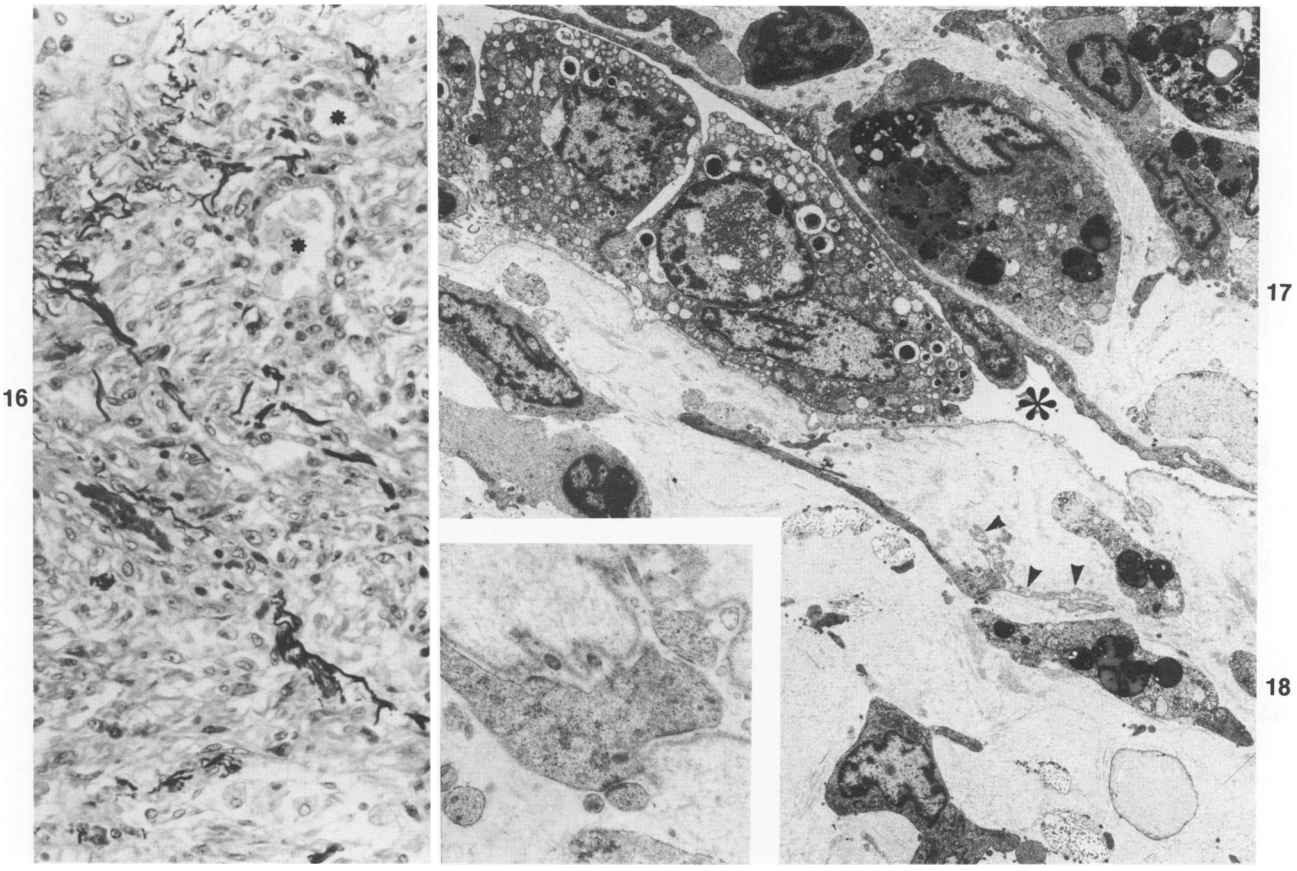

Figure 16 — Remodeled stage. The area of severe intraalveolar fibrosis is shown. Some cuboidal epithelial cells form a few small alveolar spaces *(asterisks)*. (EVG, ×200) **Figure 17** — Remodeled stage. Wavy fragmented epithelial basement membrane *(arrowheads)* is embedded in the newly formed fibrotic alveolar wall. *Asterisk* shows intraalveolar space. (×3000) **Figure 18** — High magnification of the area from Figure 17. Wavy fragmented epithelial basement membrane embedded in fibrotic tissue is attached to a myofibroblast. (×12,000)

udates. Immunohistochemistry showed that IgG, IgA, IgM, and albumin were positive in the areas of the hyaline membrane similar to that seen in the previous stages. Fibrinogen was found in the areas of hyaline membrane, and it demonstrated clearly the hyaline membrane embedded in the areas of fibrotic lesions. Fibronectin was seen predominantly in the areas of intraalveolar fibrosis. The stroma of remodeled thick alveolar walls which were covered with metaplastic squamous epithelium was frequently stained well with anti-fibronectin antibody. The basal surfaces of some squamous epithelia were linearly stained with anti-fibronectin antibody. Keratin was detected predominantly in the metaplastic squamous and cuboidal epithelium in addition to the basal cells of bronchus, bronchial glands, and mesothelium. Pulmonary surfactant apoprotein was heavily positive in increased Type II alveolar epithelial cells, the increased cuboidal cells of bronchioli, and granular materials and some hyaline membranes in intraalveolar spaces.

Electron-microscopic study showed that wavy, fragmented epithelial basement membranes were embedded in the newly formed fibrotic alveolar walls (Figure 17). These embedded epithelial basement membranes in fibrotic tissue were attached to the elongated myofibroblasts (Figure 18). The epithelial cells covering the fibrotic alveolar walls consisted of Type II and Type I alveolar epithelial cells and single-layer and stratified squamous epithelium.

Light-Microscopic Morphometry

The results of light-microscopic morphometry are shown in Figure 19. The areas of interstitium of alveolar walls were about 10% in the acute stage, and only gradually increased in later stages. On the other hand, intraalveolar fibroses were first found 7 days after the onset of clinical ARDS, and the areas of intraalveolar fibrosis were dramatically increased in the later stages. An intraalveolar fibrosis-interstitium area ratio of 3 was reached after 15 days of illness, but was approximately 1 in later stages.

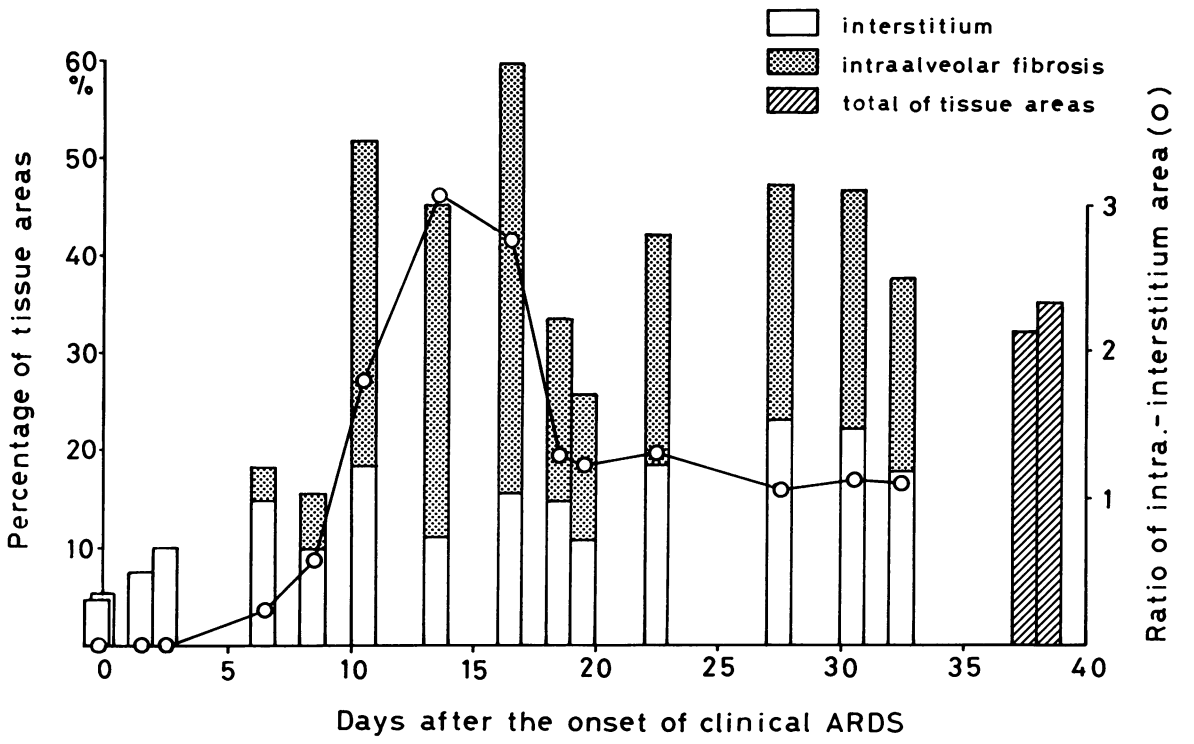

Figure 19—Changes in percentages of areas of interstitium of alveolar walls *(white column)*, and areas of intraalveolar fibrosis *(dotted column)*. Each column shows an individual case. *Open circles* show a ratio of intraalveolar fibrosis to interstitium area for each case. The areas of interstitium were gradually increased in later stages. The areas of intraalveolar fibrosis were dramatically increased after 10 days of illness. A ratio of intraalveolar fibrosis to interstitium area of 3 was reached after 15 days of illness, but was approximately 1 in later stages. After 35 days, total tissue areas *(shaded column)*, including interstitium and intraalveolar fibrosis, were measured because of the difficulty at distinguishing the areas.

Discussion

These observations confirm previous reports on the morphology of lungs in DAD.[7,14-25] This study also show, the importance of intraalveolar fibrosis in the process of pulmonary structural remodeling, in addition to fibrotic changes of lungs, in DAD. These findings also stress the importance of fibronectin in the process of intraalveolar organization. Finally, the characteristics of the metaplastic squamous epithelial cells in alveoli of lungs with DAD were demonstrated.

Pulmonary Structural Remodeling in DAD

The lungs with fibrosis resulting from DAD showed remodeled structures consisting of irregularly obliterated alveoli with varied-sized air spaces. They were similar to bronchopulmonary dysplasia resulting from idiopathic respiratory distress syndrome (IRDS) of newborn infants.[26] Although it has been reported that the fibrosis due to DAD is not only interstitial, but also intraalveolar,[2,7,24] the predominance of intraalveolar fibrosis in DAD and the role of intraalveolar fibrosis in the process of pulmonary structural remodeling have not been described. The predominance of intraalveolar fibrosis in DAD, compared with interstitial fibrosis, was shown by morphometric analysis in this study. The extensive and detailed morphometric analyses of the alveolar walls of lungs of patients with DAD[17,21,23] and oxygen-treated experimental animals[27,28] have been reported. In this study, we measured the tissue areas of organized intraalveolar areas in addition to the interstitium of alveolar walls in PAM-stained slides. In this study, the areas of interstitium of alveolar walls were increased in the acute stage, but they were edematous, not fibrotic. The percentage of the areas of interstitium were not significantly different in any of the cases. On the other hand, intraalveolar fibroses were formed rapidly in the early proliferative stage and became prominent in later stages. It is interpreted that the decrease in the ratio of intraalveolar fibrosis to interstitium area may be due to the shrinkage of the intraalveolar fibrosis. It is clear that the changes in intraalveolar fibrosis is more prominent in DAD, compared with interstitial fibrosis in this study.

The pulmonary lesions in DAD have two stages: acute and proliferative.[14] In this study the prolifera-

tive stage was divided into an early proliferative stage and a remodeled stage for the purpose of clarifying the process of the pulmonary structural remodeling. The process of the intraalveolar fibrosis in DAD is as follows: 1) epithelial cell damage, denudation, and gap formation of epithelial basement membrane; 2) activation and migration of myofibroblasts into intraalveolar spaces through the gap of epithelial basement membrane; 3) attachment of migrated myofibroblasts to the luminal side of the epithelial basement membrane; and 4) production of extracellular elements of connective tissue within the intraalveolar spaces. So the alveolar spaces are partially or completely obliterated, and the apposed alveolar walls of the collapsed alveoli undergo fusion or coalescence. This was similar to the experimental study of monkeys with paraquat intoxication,[6] although in the experimental study of monkeys, migrating cells were fibroblastic and later changed to myofibroblasts or smooth muscle cells in the intraalveolar spaces. It was confirmed that intraalveolar fibrosis was essential in remodeling the lungs in human cases of DAD.

It has been reported that three patterns of intraalveolar fibrosis — 1) intraluminal buds, 2) obliteration of alveoli, and 3) mural incorporated lesions to alveolar walls, are frequently found in various types of fibrotic lung disorders.[13] In DAD, Patterns 2 and 3 were frequently found. It is interpreted that epithelial cell damage is very severe in DAD. The variations of intraalveolar fibrosis may result from the correlation of the invaded and proliferated interstitial cells in intraalveolar spaces and the regenerating epithelial lining cells. The activation, migration and proliferation of these interstitial cells and the regeneration of epithelial cells in alveoli might depend on the various chemotactic and growth factors released by activated macrophages and other inflammatory cells.[29]

The Definition of Deposition of Several Kinds of Plasma Proteins and Pulmonary Surfactant Apoprotein in Intraalveolar Spaces Including Hyaline Membrane

In the acute stage of DAD, severe proteinaceous edema and hyaline membrane formation are found. It has been suggested that the plasma protein in intraalveolar spaces results from the increased permeability of alveolar wall vessels due to the alveolar wall damage.[30,31] In this study, albumin, surfactant apoprotein, fibrinogen, and immunoglobulins, especially IgG, are frequently found in the areas of hyaline membrane by immunohistochemistry. On the other hand, complements were usually not detected in alveoli in lungs with DAD. The specific antibody activity against normal lung tissues was not detected in the supernatant fluid after centrifugation of homogenates of lung tissues of some cases of DAD (Ishizaki and Fukuda, unpublished data). It is speculated that the immunoglobulins in hyaline membrane are the nonspecific accumulation from plasma.

The pattern of distribution of fibronectin in intraalveolar spaces was different from the previously mentioned plasma proteins in this study. In the acute stage, fibronectin was detected scantily on the surfaces of the hyaline membrane. In later stages, fibronectin was predominantly found on the surfaces of hyaline membranes and the areas of intraalveolar fibrosis.

Alveolar macrophages from fibrotic lung disorders produce increased amounts of fibronectin.[32] Fibronectin acts not only as a chemotactic factor[33] but also as a growth factor for fibroblasts,[34] and it facilitates fibroblast attachment to connective tissue components.[35] It is speculated that at least some part of fibronectin of intraalveolar spaces in the acute stage of DAD may be produced by alveolar macrophages *in situ* and is added, later, to the hyaline membrane. Fibronectin may be responsible for the recruitment and migration of the myofibroblasts into intraalveolar spaces and proliferation in intraalveolar spaces. In fact, myofibroblasts did not penetrate into hyaline membranes themselves, but covered them.

The surfactant apoprotein was predominantly found in intraalveolar spaces as granular material and in the hyaline membranes in DAD. It was confirmed that the hyaline membranes included surfactant apoprotein and exuded plasma protein in the cases of DAD. The cases having much accumulation of pulmonary surfactant apoprotein in the intraalveolar spaces usually showed marked increases of Type II alveolar epithelial cells, which were stained heavily in their cytoplasm by the DAB reaction for surfactant apoprotein. Autopsy cases of IRDS in premature babies showed no or only trace amounts of surfactant apoprotein in hyaline membranes and intraalveolar spaces.[36] This is in contrast to the finding in cases of DAD in this study, which have been diagnosed clinically as ARDS. The main cause of IRDS in premature babies is considered to be a deficiency of surfactant.[37,38] IRDS in premature babies has been treated with artificial surfactants with satisfactory results.[39] It is speculated that the large amount of surfactant in intraalveolar spaces of lungs in ARDS is ineffective in improving respiratory failure, because the damage of alveolar walls, especially in vessels, may be most severe in ARDS, compared with IRDS in premature babies.

Characteristics of the Metaplastic Squamous Epithelial Cells in Alveoli in Lungs of DAD

The morphologic characteristics of regenerating epithelial cells in alveoli in the early proliferative and remodeled stages are metaplastic single-layer and stratified squamous epithelial cells in addition to Type II alveolar epithelial cells. Metaplastic squamous epithelium was frequently found in the areas of severe intraalveolar fibrosis, especially single-layer metaplastic squamous epithelium, which covered widely the intraalveolar fibrosis. It has been suggested that the severe epithelial cell damage and lesser regeneration of Type II cells after the alveolar wall damage may be one of the factors that produce the intraalveolar fibrosis,[6] and metaplastic squamous epithelium later covers these lesions.

The origin of the squamous metaplastic epithelial cells in alveoli is controversial. Both metaplastic single-layer and stratified squamous epithelial cells in fibrotic alveoli were surfactant apoprotein-negative and heavily keratin-positive. The staining patterns of surfactant apoprotein and keratin in control lungs in this study were similar to those in previous reports.[40,41] One possible mechanism is that these metaplastic epithelia originate from the bronchial basal cells.

Alveolar epithelial cells having cytoplasmic hyaline were first described in patients exposed to asbestos.[42] Katzenstein and Askin[7] described this cytoplasmic hyaline in alveolar epithelial cells in patients with DAD. Warnock et al[43] have reported that cytoplasmic hyaline is not specific for asbestosis but is a nonspecific reaction to injury and have speculated that these cells having cytoplasmic hyaline probably originate from Type II alveolar epithelial cells, because of the occasional ultrastructural findings of similar cells containing Type II cell lamellar inclusions but lacking hyaline. We suspect that cells having cytoplasmic hyaline are regressing cells originating from the single-layered squamous metaplastic cells in alveoli. This is supported by data which show that they do not always have any surfactant apoprotein and lamellated inclusions in their cytoplasm and are located with stratified and single-layer squamous epithelial cells. They also frequently protrude into the intraalveolar spaces and attach only with thin cytoplasmic processes to other epithelial cells or to the epithelial basement membrane.

In conclusion, intraalveolar fibrosis appears to be an essential factor in the remodeling of lungs in patients with DAD. Intraalveolar fibrosis might be important in the formation of the remodeled lungs not only in DAD but also in various other fibrotic lung disorders.

References

1. Kuhn C, Askin FB, Katzenstein AA: Diagnostic light and electron microscopy, Lung Biology in Health and Disease. Vol 16, Diagnostic Techniques in Pulmonary Disease. Part 1. Edited by MA Sackner. Basel, Marcel Dekker, 1980, pp 89–202
2. Katzenstein AA, Askin FB: Chronic interstitial pneumonia, interstitial fibrosis, and honeycomb lung, Major Problems in Pathology. Vol 13, Surgical Pathology of Non-neoplastic Lung Disease. Philadelphia, W.B. Saunders Company, 1982, pp 43–72
3. Kawanami O, Ferrans VJ, Crystal RG: Structure of alveolar epithelial cells in patients with fibrotic lung disorders. Lab Invest 1982, 46:39–53
4. Spencer H: Pathogenesis of interstitial fibrosis of the lungs. Progr Respir Res 1975, 8:34–44
5. Basset F, Lacronique J, Ferrans VJ, Fukuda Y, Crystal RG: Intraalveolar fibrosis: A second form of fibrosis of the interstitial lung disorders (Abstr). Am Rev Respir Dis 1984, 129 (Part II):A-72
6. Fukuda Y, Ferrans VJ, Schoenberger CI, Rennard SI, Crystal RG: Patterns of pulmonary structural remodeling after experimental paraquat toxicity: The morphogenesis of intraalveolar fibrosis. Am J Pathol 1985, 118:452–475
7. Katzenstein AA, Askin FB: Diffuse alveolar damage,[2] pp 9–42
8. Mapp PI, Mayston VJ, Revell PA: Apparent staining of mast cells for fibronectin with a peroxidase-antiperoxidase method for formalin fixed sections. J Immunol Methods 1984, 71:107–110
9. Engvall E, Ruoslahti E: Binding of soluble form of fibroblast surface protein, fibronectin, to collagen. Int J Cancer 1977, 20:1–5
10. Kuroki T, Fukada Y, Takahashi H, Akino T: Monoclonal antibodies against human pulmonary surfactant apoprotein: Specificity and application in immunoassay. Biochim Biophys Acta 1985, 836:201–209
11. Graham RC, Karnovsky MJ: The early stages of absorption of injected horseradish peroxidase in the proximal tubules of mouse kidneys: Ultrastructural cytochemistry by a new technique. J Histochem Cytochem 1966, 14:291–302
12. Kajikawa K, Yamaguchi T, Katsuda S, Miwa A: An inproved electron stain for elastic fibers using tannic acid. J Electron Microsc (Tokyo) 1975, 24:287–289
13. Basset F, Ferrans VJ, Soler P, Takemura T, Fukuda Y, Crystal RG: Intraluminal fibrosis in interstitial lung disorders. Am J Pathol 1986, 122:443–461
14. Nash G, Blennerhassett JB, Pontoppidan H: Pulmonary lesions associated with oxygen therapy and artificial ventilation. N Engl J Med 1967, 276:368–373
15. Soloway HB, Castillo Y, Martin AM: Adult hyaline membrane disease: Relationship to oxygen therapy. Ann Surg 1968, 168:937–945
16. Gould VE, Tosco R, Wheelis RF, Gould NS, Kapanci Y: Oxygen pneumonia in man: Ultrastructural observations on the development of alveolar lesions. Lab Invest 1972, 26:499–508
17. Kapanci Y, Tosco R, Eggermann J, Gould VE: Oxygen pneumonitis in man: Light and electron-microscopic morphometric studies. Chest 1972, 62:162–169
18. Anderson WR, Strickland MB, Tsai SH, Haglin JJ: Light microscopic and ultrastructural study of the adverse effects of oxygen therapy on the neonate lung. Am J Pathol 1973, 73:327–348
19. Sevitt S: Diffuse and focal oxigen pneumonitis: a preliminary report on the threshold of pulmonary oxygen toxicity in man. J Clin Pathol 1974, 27:21–30
20. Nash G, Langlinais PC: Pulmonary interstitial edema and hyaline membranes in adult burn patients: Elec-

tron mecroscopic observations. Human Pathol 1974, 5:149–160
21. Bachofen M, Weibel ER: Basic pattern of tissue repair in human lungs following unspecific injury. Chest 1974, 65:14s–21s
22. Katzenstein AA, Bloor CM, Liebow AA: Diffuse alveolar damage- the role of oxygen, shock, and related factors. Am J Pathol 1976, 85:210–228
23. Bachofen M, Weibel ER: Alterations of the gas exchange apparatus in adult respiratory insufficiency associated with septicemia. Am Rev Resp Dis 1977, 116:589–615
24. Zapol WM, Trelstad RL, Coffey JW, Tsai I, Salvador RA: Pulmonary fibrosis in severe acute respiratory failure. Am Rev Respir Dis 1979, 119:547–554
25. Pratt PC, Vollmer RT, Shelburne JD, Crapo JD: Pulmonary morphology in a multihospital collaborative extracorporeal membrane oxygenation project: 1. Light microscopy. Am J Pathol 1979, 95:191–214
26. Northway WJr, Rosan R, Porter D: Pulmonary disease following respiratory therapy of hyaline-membrane disease. Bronchopulmonary dysplasia. N Engl J Med 1967, 276:357–368
27. Kistler GS, Caldwell PRB, Weibel ER: Development of fine structural damage to alveolar and capillary lining cells in oxygen-poisoned rat lungs. J Cell Biol 1967, 33:605–628
28. Kapanci Y, Weibel ER, Kaplan HP, Robinson FR: Pathogenesis and reversibility of the pulmonary lesions of oxygen toxicity in monkeys: II. Ultrastructural and morphometric studies. Lab Invest 1969, 20:101–118
29. Crystal RG, Bitterman PB, Rennard SI, Hance AJ, Keogh BA: Interstitial lung diseases of unknown cause: Disorders characterized by chronic inflammation of the lower respiratory tract. N Engl J Med 1984, 310:154–166; 235–244
30. Birke G, Liljedahli O, Plantin O: Distribution and losses of plasma proteins during the early stage of severe burns. An NY Acad Sci 1968, 150:895–904
31. Fein A, Grossman RF, Jones JG, Overland E, Pitts L, Murray JF, Staub NC: The value of edema fluid protein measurement in patients with pulmonary edema. Am J Med 1979, 67:32–38
32. Schoenberger CI, Rennard SI, Bitterman PB, Fukuda Y, Ferrans VJ, Crystal RG: Paraquat-induced pulmonary fibrosis-Role of the alveolitis in modulating the development of fibrosis. Am Rev Respir Dis 1984, 129:168–173
33. Rennard SI, Hunninghake GW, Bitterman PB, Crystal RG: Production of fibronectin by the human alveolar macrophages: Mechanism for recruitment of fibroblasts to sites of tissue injury in interstitial lung diseases. Proc Natl Acad Sci USA 1981, 78:7147–7151
34. Bitterman PB, Rennard SI, Adelberg S, Crystal RG: Role of fibronectin as a growth factor for fibroblasts. J Cell Biol 1983, 97:1925–1932
35. Klebe RJ: Isolation of a collagen-dependent cell attachement factor. Nature 1974, 250:248–251
36. Akino T, Kuroki Y, Takahashi H, Dempo K: Monoclonal antibodies against human pulmonary surfactant apoproteins: Its application in immunoassay and immnohistochemistry. J Jpn Soc Biol Interface (Tokyo) 1985, 16:111–125
37. Avery ME, Mead J: Surface properties in relation to atelectasis and hyaline membrane disease. Am J Dis Child 1959, 97:517–523
38. Adams FH, Fujiwara T, Emmanouilides G, Raiha H: Lung phospholipid of human fetuses and infants with and without hyaline membrane disease. J Pediatr 1970, 77:833–841
39. Fujiwara T, Maeta H, Chida S, Morita T, Watabe Y, Abe T: Artificial surfactant therapy in hyaline-membrane disease. Lancet 1980, 1:55–59
40. Balis JU, Paterson JF, Paciga JE, Haller EM, Shelley SA: Distribution and subcellular localization of surfactant-associated glycoproteins in human lung. Lab Invest 1985, 52:657–669
41. Schlegel R, Banks-Shlegel S, Pinkus GS: Immunohistochemical localization of keratin in normal human tissues. Lab Invest 1980, 42:91–96
42. Kuhn C, Kuo T-T: Cytoplasmic hyaline in asbestosis: A reaction of injured alveolar epithelium. Arch Pathol Lab Med 1973, 95:190–194
43. Warnock ML, Press M, Churg A: Further observations on cytoplasmic hyaline in the lung. Human Pathol 1980, 11:59–65

Acknowledgments

The authors wish to thank Dr. Y. Kuroki and Dr. T. Akino for providing anti-surfactant apoprotein antibody and Mr. T. Arai for skilled technical assistance. They also wish to express their appreciation to Dr. M. Ghazizadeh and Mr. T. Shiratori for preparation of the manuscript.